7

Bolometers for Fusion Plasma Diagnostics

Kumudni Tahiliani and Ratneshwar Jha
Institute for Plasma Research,
India

1. Introduction

The thermonuclear fusion is one of the most seriously pursued alternative sources of energy for the future of mankind. The fusion energy is safer and cleaner compared to fission energy, produces no greenhouse gases and, the nuclear fuels are evenly distributed throughout the globe. Nuclear fusion is responsible for heat and radiation generated by the Sun. In the Sun, two atoms of hydrogen fuse together to produce helium. It has been determined that the fusion of the two hydrogen isotopes, namely deuterium (D) and tritium (T) that produces 17.6 MeV (mega electron-volt) of fusion energy, is feasible in a laboratory setting (Wesson, 2004). The D-T fusion however takes place at fairly high temperature of 10-30 keV or, (1-3) $\times 10^7$ K, which is necessary for deuterium and tritium nuclei to come close together to overcome electrostatic repulsion. At these thermonuclear temperatures, the atoms get stripped of all the electrons and form a plasma (electrically charged gas). Such plasmas can be confined in a desired region by using strong magnetic fields. The magnetic fields force the particles to spiral along the field lines thus confining them. The most promising magnetic confinement systems are toroidal in shape. Among the toroidal shaped plasma devices, tokamak is the most advanced one. Presently, ITER (International Thermonuclear Experimental Reactor) is the largest tokamak under construction at Cadarache, France, and JET (Joint European Torus) in Culham, UK is the largest operating tokamak. Other non-magnetic confinement systems are also being investigated. For example, the laser induced inertial confinement systems.

One of the main requirements of the fusion plasmas is to heat the plasma particles to very high temperatures. The typical power required to attain the thermonuclear temperatures in ITER is approximately 50 megawatt (Shimada et al., 2007). The heating methods employed to heat the plasma to these temperatures are ohmic heating, neutral beam heating, and radiofrequency (RF) heating. In order to ohmically heat the plasma, a current of the order of millions of amperes is induced in the plasma. The current heats the plasma through the acceleration of charged particles and provides few megawatts of power. In the neutral beam heating method, a beam of energetic neutral particles of the working gas heats the plasma particles by momentum transfer. This provides power of the order of tens of megawatts. Radio frequency heating involves injection of RF power, either matching with the ion cyclotron frequency or the electron cyclotron frequency. This method also provides heating power of the order of 10 megawatts. Apart from temperature, there are other conditions on the density and the confinement time of fusion plasma, which comes from the breakeven criterion for the feasibility of nuclear fusion for energy production. The required conditions are ion density of 1-2 $x10^{20}$ m^{-3} and confinement time of 4-6 seconds. The confinement time

depends on several loss mechanisms through which the power is lost from the plasma. For example, plasma energy is lost through fast neutrals resulting from the charge exchange processes of plasma ions that cannot be confined by the magnetic field, through the cross-field diffusion of charged particles, and through radiation from the impurities present in the plasma. The radiation power loss is a significant fraction of the total power loss and reaches 100% in certain plasma regimes.The impurities that contribute to the radiation power loss from the plasma are low z (hydrogen, carbon, and oxygen), medium z (iron, molybdenum and silicon), and high z (tungsten). The low z impurities enter the plasma by low energy detachment processes of molecules adsorbed on the machine walls. Whereas, sputtering, arcing and evaporation processes from the wall or plasma facing components release medium and high z impurities. If the concentrations are large enough, these impurities may radiate enough power through spectral lines of incompletely stripped ions to degrade the plasma energy confinement. Ignition of D-T plasmas can be prevented by the presence of only 3% of low z-elements (oxygen), 1% of intermediate z element (iron), or 0.1% of high z element (tungsten) (Jensen et al., 1997). So it is essential to measure and control the radiation power loss in fusion plasmas. The radiated power measurement is also needed in power balance calculations, in the study of ion and electron transport processes, and also to study the interaction of plasma with walls and limiter. Some physical phenomena, for example, plasma disruptions, radiative instabilities, and detached plasmas are studied using the power loss measurements.

The radiation power loss from tokamak plasma is measured using bolometers. Bolometers are detectors that can measure radiation over a broad spectrum, from the soft x-rays to the infrared, with a nearly uniform responsivity at all wavelengths. The bolometers are used in two types of configurations in tokamaks. In the first type, a single bolometer is placed behind a pinhole and it views the whole poloidal section of the plasma from one toroidal location. This gives the total power radiated from the plasma since the tokamak plasmas are toroidally symmetric. In the second configuration, a linear array of bolometers is placed behind a single pinhole, each bolometer looking at different region of the plasma. These measurements are inverted to obtain the radiation emission distribution in the plasma.

The operational requirements of bolometers in tokamak plasmas are high sensitivity, small area for optimal spatial resolution (few mm in edge plasmas), in-situ calibration, fast time response (less than few ms), ultra-high vacuum compatibility, and high electromagnetic fields and high temperature compatibility. The tokamaks are equipped with huge systems like magnets both for confinement and for equilibrium, limiters, diverters, heating systems, and gas puff systems. These systems are spread on and around the tokamak. This renders a very limited space for diagnostics and a limited access to the ports. Difficulty to access the bolometers after mounted inside requires bolometers to be reliable over a long period of operation. The bolometers should also meet radiation hardness requirement to prevent damage by neutron and gamma radiation in present and next generation fusion devices.

Different kinds of bolometers have been tested in tokamaks for radiation power loss measurements. Bolometers used in currently operating fusion plasmas have evolved from the ones used in other non-fusion plasmas. These bolometers need some changes to adapt in future fusion devices. Following section briefly discusses all kinds of radiation sensors/detectors that have been used in the plasma devices for radiated power measurements. It describes in detail the detectors that are used in currently operating devices. The section also evaluates feasibility of such detectors for use in next generation fusion devices.

2. Types of bolometers

In the earlier tokamaks, the radiation was measured using thermal detectors. A thermal detector absorbs radiation that in turn changes its physical property. It is also sensitive to the particle flux. So, in addition to the radiation, thermal detectors also measure the energy loss from neutral and charged particles. Thermopiles and pyroelectric detectors are two types of thermal detectors that have been used in tokamaks. Bolometer refers to the kind of thermal detector in which the temperature change produced by the absorption of radiation and particle flux causes a change in the electrical resistance of the detector material. Thermistor, semiconductor, and metal foil are the types of bolometers that have been used in tokamaks. AXUV (Absolute Extreme Ultra Violet) detectors and IR (Infra Red) detectors are fairly new techniques for measuring the radiated power. AXUV detectors are photodiodes that measure the current induced by the incident radiation. Whereas, IR detectors measure the IR radiation emitted by the metal foil placed in the line of sight of the incident radiation.

2.1 Thermopiles

Thermopiles have several thermocouples, connected in series. Its principle of operation is same as of a thermocouple. The most commonly used materials for a thermopile are antimony and bismuth, which give the best seebeck coefficient. The responsivity of a thermopile is given by,

$$R_{res} = \frac{n\alpha\varepsilon}{\kappa} \tag{1}$$

where, n is the number of thermocouples, α is the seebeck coefficient, ε is the detector emissivity and κ is the thermal conductance. The typical responsivity is 5-15 V/W and the time response is few milliseconds (Sharp et al., 1974). They have been used in ORMAK (Edmunds and England, 1978) and DITE tokamaks. Although the responsivity of thermopiles is high, it has a slow response time and very sensitive to radiation damage. Therefore, thermopiles are not suitable for use in fusion plasmas.

2.2 Pyroelectric detector

Pyroelectric detectors are made of ferroelectric single crystals that have permanent electrical polarization. The temperature of the material affects the degree of this polarization, and a change in the surface charge results from a change in temperature, which can be measured through an external circuit. Lithium niobate or tantalate ($LiNbO_3$ or $LiTaO_3$), deuterated triglycine sulfate (DTGS), strontium barium niobate, and polyvinylidene fluoride are some of ferroelectric materials. The current induced is given by,

$$I = \rho(T) A \frac{dT}{dt} \tag{2}$$

where, ρ(T) is the pyroelectric coefficient, A is the sensing area, and dT/dt is the rate of temperature change. Pyroelectric detectors can directly measure differential radiation power. But there is a need for a preamplifier near the detector. Also it is sensitive to radiation damage, which begins to take effect from a 1 MeV neutron fluence of ~ 5×10^{14} n-cm^2 (Orlinskiz and Magyar, 1988). These detectors have been used in DIVA (Odajima et al.1978), ISX-B (Bush and Lyon, 1977) and TFR (TFR groups, 1980) tokamaks.

2.3 Thermistor

Thermistors are made of materials that have a high temperature coefficient of resistance. They include germanium and oxides of manganese, cobalt, or nickel. The absorbing element is made by sintering wafers of these materials together and mounted on an electrically insulating but thermally conducting material such as sapphire. The incident radiation increases the temperature of the thermistor, hence, decreasing the resistance. Thermistors are highly sensitive and have been used in Alcator A (Scaturro and Pickrell, 1980), PBX (Paul et al., 1987), and ATC (Hsuan et al., 1975) tokamaks. But they are damaged by even a relatively small dose of neutrons and gamma rays (~10^7 rad) (Schivell, 1982).

2.4 Semiconductor foil bolometer

Semiconductor foil bolometers consist of a metallic absorber foil and a semiconductor detector film connected together by a thermally conducting and electrically insulating substrate. Under normal operation, an accurately controlled bias current is passed through the resistor element. Thus for a radiation input causing a change in the bolometer resistance, there is an output voltage,

$$\Delta V = IR_0(1 - \exp(-\alpha \Delta E / C)) \tag{3}$$

Here, R_0 is semiconductor resistance at 0 °C, α is temperature coefficient of resistance (4-5 % K^{-1}), ΔE is absorbed energy, and C is heat capacity of the multilayer foil. These bolometers have been used in TM-2, TM-3 (Gorelik et al., 1972), JFT-2 (Maeno and Katagiri, 1980), and TCA (Joye and Marmillod, 1986) tokamaks. Despite their high sensitivity, these bolometers are prone to radiation damage.

2.5 Metal foil bolometer

A typical metal foil bolometer is composed of three layers: a metallic absorber layer, a thermally conducting but electrically insulating substrate layer, and a metallic resistor layer (see figure (1)). The absorber layer absorbs the incident radiation, which causes a rise in its temperature. The heat is conducted through the substrate layer to the resistor layer, which increases its temperature and hence the resistance. The change in resistance is measured electrically and is related to the incident power.

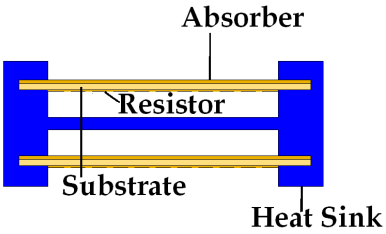

Fig. 1. Schematic of metal foil bolometer configuration, showing the measuring and the reference bolometer.

The absorber layer is made of metal, which is either gold or platinum. These metals have nearly constant absorption from 2000Å up to soft x-rays and a high reflectivity for

wavelengths below 2000Å (Sabine, 1939). The substrate layer made of either mica or kapton provides mechanical strength to the bolometer and electrically insulates the absorber layer from the resistor layer. The resistor layer is of the same metal as the absorber layer and is made in the form of a meander to have a high resistance (~ few kΩ). The whole foil is in contact with a lateral heat sink.

The thickness of the metal foil bolometer is a compromise between two opposing requirements: (1) the absorber layer has to be thick enough to absorb the highest energy radiation expected from the plasma, and (2) the total thickness of the bolometer has to be small in order to increase sensitivity and decrease response time. The typical thickness of the absorber layer is 3-4 μm, of the substrate layer is around 7 μm, and that of the resistor layer is around 0.01μm.

To compensate for temperature drifts and electromagnetic interferences, a second reference bolometer, shielded from incident plasma radiation, is used. A reference meander and another measurement resistor are coupled in a bridge circuit such that the output voltage is proportional to the temperature change of the measuring bolometer.

2.5.1 Metal foil bolometer signal analysis

If a radiation power P is uniformly incident on bolometer foil, the temporal evolution of the temperature is governed by the differential equation (Mast et al., 1991),

$$P = C\left(\frac{dT}{dt} + \frac{T}{\tau_c}\right) \tag{4}$$

Here, C (= A $c_p \rho d$) is heat capacity of the foil and τ_c is the cooling time constant, which is a measure of heat loss rate to the heat sink. The radiation losses have been omitted since the detector temperature is close to the ambient temperature for most of the cases. Also, a uniform profile has been assumed on the foil.

The frequency response of the bolometer is given by,

$$T(\omega) = \frac{P(\omega)}{C}\frac{\tau_c}{\sqrt{1+\omega^2{\tau_c}^2}} \tag{5}$$

Thus, at a fixed incident power P(ω), the temperature is inversely proportional to the heat capacity. So the bolometer thickness should be minimum for a higher signal level. Also, when the frequency is low i.e. $\omega\tau_c << 1$, the temperature amplitude is given by,

$$T(\omega) = \frac{P(\omega)}{C}\tau_c \tag{6}$$

Thus, the temperature grows linearly with τ_c at low frequencies. At high frequencies of the input power ($\omega\tau_c >> 1$)

$$T(\omega) = \frac{P(\omega)}{C\omega} \tag{7}$$

In this case, the temperature is inversely proportional to the input frequency and the thermal insulation of the bolometer foil has no effect on the signal to noise ratio.

In equation (4), a uniform incident power as well as uniform temperature distribution on the foil was assumed, which is not true in the actual case. The heat conduction to the sink results in losses and a non-uniform temperature distribution. This heat conduction is in X-Y-Z direction but since the thickness of the bolometer is very small compared to the area, a two-dimensional treatment of heat conduction is sufficient. The heat diffusion equation for the bolometer can be written as (Mast et al., 1991),

$$\mathrm{P(x,y,t)} = \mathrm{C}\left[\frac{\partial \mathrm{T(x,y,t)}}{\partial \mathrm{t}} - \mathrm{D}\left(\frac{\partial^2}{\partial \mathrm{x}^2} + \frac{\partial^2}{\partial \mathrm{y}^2}\right)\mathrm{T(x,y,t)}\right] \tag{8}$$

Here D, is the thermal diffusivity. For a square foil of side 2a, T can be expanded in terms of double Fourier series, with mode numbers (l, m).

$$\mathrm{T(x,y,t)} = \sum_{\mathrm{l}}\sum_{\mathrm{m}} \mathrm{T_{l,m}(t)}\cos\left[(2\mathrm{l}+1)\frac{\pi \mathrm{x}}{2\mathrm{a}}\right] \times \cos\left[(2\mathrm{m}+1)\frac{\pi \mathrm{y}}{2\mathrm{a}}\right] \tag{9}$$

Similarly, we can write P as,

$$\mathrm{P(x,y,t)} = \sum_{\mathrm{l}}\sum_{\mathrm{m}} \mathrm{P_{l,m}(t)}\cos\left[(2\mathrm{l}+1)\frac{\pi \mathrm{x}}{2\mathrm{a}}\right] \times \cos\left[(2\mathrm{m}+1)\frac{\pi \mathrm{y}}{2\mathrm{a}}\right] \tag{10}$$

Using above equations, we get the following solution for equation (8),

$$P_{l,m}(t) = C\left[\frac{d}{dt}T_{l,m}(t) + \frac{T_{l,m}(t)}{\tau_{l,m}}\right] \tag{11}$$

where,

$$\tau_{l,m} = \frac{\tau_{00}}{2\left((2l+1)^2 + (2m+1)^2\right)} \tag{12}$$

Time constant τ_{00} corresponds to the fundamental mode of the series expansion. The fundamental Fourier mode (0,0) contributes maximum to the solution with rest of the modes up to (2,2) making some contribution (up to 3%) to the sum. Considering only the fundamental mode and assuming constant radiation power, the solution is same as equation (4).

Using equation (4), the temperature of the foil can be written as,

$$T = \frac{P\tau_c}{C}\left(1 - e^{-t/\tau_c}\right) \tag{13}$$

The temperature increase causes an increase in the resistance of the metal given by,

$$\Delta R = R_0 \alpha \Delta T \tag{14}$$

which is measured using a standard Wheatstone bridge (Schivell et al., 1982).

2.5.2 Calibration procedures

A well developed method is required to calibrate the detectors in order to determine their physical properties of use. The aim of the calibration procedures in the metal foil bolometers is to determine the value of the heat capacity C and the cooling time constant τ_c. This is done in two stages. First, a known constant power P is made incident on the detector, which raises the temperature of the foil to a saturation value, T_{sat}. The power and the T_{sat} measurements give the value of ratio τ_c /C, which is also called the thermal resistance (z) of the bolometer,

$$z = \frac{\tau_c}{C} = \frac{T_{sat}}{P} \tag{15}$$

In the second stage, the bolometer surface is uniformly irradiated by using a radiation pulse and then the radiation power source is turned off. This results in the exponential decay of the temperature, known as the cooling curve. From the cooling curve of the bolometer, τ_C is determined using Eq. (13). Using the measured values of τ_C and z, the value of C is determined.

The metal foil bolometer is presently the most widely used detector in tokamak plasmas. It has been used in TFTR (Schivell et al., 1982), ASDEX (Muller and Mast, 1984), JET (Mast et al., 1985) and TEXT (Snipes et al., 1984) tokamaks. Table 1 lists the metal foil bolometer characteristics for JET and ASDEX tokamaks. Metal foil bolometer has been used in D-T plasmas and has shown resistance to radiation up to 10 Grad. The metal foil bolometer is the potential candidate for ITER tokamak, and it is being tested for the expected radiation and neutron flux levels.

Bolometer foil characteristics	JET (Mast et al., 1985)	ASDEX (Muller and Mast, 1984)
Heat capacity C (mJ K^{-1})	2.2	2
Cooling time constant τ_C (s)	0.2	0.173
Heat resistance $z = \tau_C / C$ (K/W)	90	90
Detection limit ($\mu W/cm^{-2}$)	70	100
Response time (ms)	1	1
Resistance R (kΩ)	4.8	5
Resistance temperature coefficient α ($\Delta R/\Delta T x 1/R$)(K^{-1})	2.7 x 10^{-3}	2.5 x 10^{-3}
Response dV/dP (I = 1mA) (V/W)	0.5	1.2
Integration time τ_{int} (ms)	20	10
Foil size	11 x 11 (mm^2)	10 x 10 (mm^2)
Baking temperature (°C)	150	150
Neutron fluence cm^{-2}	2.5 x 10^{14}	2.5 x 10^{14}
Radiation dose (rad)	1 x 10^{10}	1 x 10^{10}
Foil/substrate	Gold/Kapton	Gold/Kapton

Table 1. Metal foil bolometer parameters in JET and ASDEX.

2.6 AXUV detectors

AXUV detectors are special kind of photodiodes that have a uniform response from the ultraviolet up to the soft x-ray energies. Their basic operation is similar to a photodiode. When a photon of energy $h\nu > E_g$ (band gap energy) is incident on a photodiode, electron-hole pairs are produced and are swept apart by the internal electric field at the p-n junction. This generates a current, which is called photocurrent. The upper wavelength detection limit is determined by the attenuation coefficient of the material of the photodiode and the thickness while the lower limit is governed by the reflection and the absorption in the oxide layer at the top.

AXUV detectors are n- on p- type photodiodes with a thin silicon dioxide (SiO_2) layer and a fully depleted active region. This configuration has an advantage over the p- on n- configuration. Radiation also generates electron-hole pairs in the oxide layer. These holes accumulate close to the SiO_2/Si interface, leading to a positive charge of the oxide. This charge attracts electrons created in the bulk towards the p-doped layer adjoining the SiO_2/Si interface, where the recombination probability is higher. This results in lower responsivity. To avoid this loss, the diode structure is inverted (n on p). The positive oxide charge created in irradiation repels the electrons from the SiO_2/Si interface, thus supporting the charge carrier drift in the n-p junction when the oxide is attached to the n doped layer.

The cross section of AXUV photodiode is shown in figure (2) (Korde, 2007). The top-most layer of the device is an active oxide region (SiO_2), which acts both as an antireflection coating and a passivation layer to protect the diode. This layer is made very thin (3-7 nm) in order to reduce losses at lower wavelengths. This is very crucial since below 700 eV, a great part of the incident radiation is absorbed in the first several hundred nanometers of a semiconductor detector (Krumery and Tegeler, 1990). If a photon is absorbed in the oxide layer, possibly there is no contribution of the charge generated to the external current due to the absence of an electric field. A thin oxide layer minimizes these losses. The oxide layer in AXUV detector is also nitrided for radiation hardness of 1 Grad.

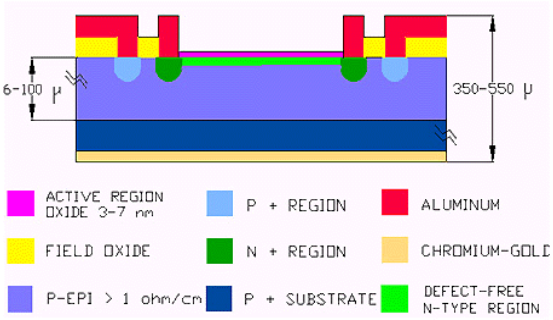

Fig. 2. The cross-section of AXUV photdiode.

2.6.1 AXUV photodiode characteristics

A photodiode performance is characterized by two parameters: the quantum efficiency (η) and the responsivity (R_{res}). Quantum efficiency is the number of electron hole pairs generated per incident photon. It is given by,

$$\eta = \frac{E_{ph}}{E_g} \tag{16}$$

where, E_{ph} is the energy of the incident photon and E_g is the band gap energy. Since the band gap energy (also called mean electron hole pair energy) is independent of the energy of the absorbed radiation, the quantum efficiency of an ideal semiconductor should linearly increase with the photon energy. A typical quantum efficiency plot of AXUV diode is shown in Figure 3. As shown, η is linear for energies above 100 eV (Check this number, as SiO2 band gap is below 20). This value can be derived theoretically from equation (16) using E_g = 3.66 eV for silicon (although the band gap energy is 1.1 eV in silicon, since it is an indirect semiconductor, an electron in the valence band goes to conduction band only if a phonon participates in the process. Hence the energy needed for creation of one electron hole pair is 3.66 eV). Below 100 eV, there is a significant loss in the quantum efficiency due to absorption of radiation in the oxide layer and reflection from the surface.

The second and important characteristic of a photodiode is its responsivity. It is defined as the current produced by the photodiode per unit incident power, and s given by:

$$R_{res} = \frac{I}{P} \tag{17}$$

Here, I is the photocurrent produced by incident power, P. The quantum efficiency and responsivity are related to each other as,

$$R_{res} = \frac{\eta e}{h\nu} \tag{18}$$

The responsivity curve of the AXUV photodiode is also shown in figure 3. The diode has a high reponsivity (0.27 A/W) at high energies and an average responsivity of 0.24 A/W above 100 eV. Below 100 eV, R_{res} varies significantly and drops down to 0.12 A/W at 10 eV.

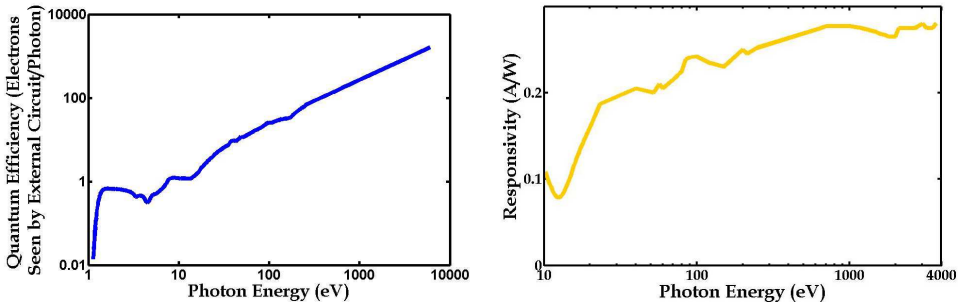

Fig. 3. Quantum efficiency (left) and the responsivity curve (right) of AXUV photodiode (Korde, 2007).

Because the response of the AXUV photodiode varies significantly at low energies, for the estimation of total radiated power from a tokamak, an effective responsivity value is determined. For this purpose the power contribution of different wavelengths to the measured is determined using different filters (Gray et al., 2004).

The response time of an AXUV bolometer is of the order of a fraction of μs. The AXUV photodiodes are ultra high vacuum compatible and can survive high baking temperatures without any significant change of properties. They can be miniaturized and made into arrays. They are also radiation hard and can survive up to 1 Grad. AXUV photodiodes have been used in TEXT-U (Wen and Brevenec, 1995), TCV (Ferno et al., 1999), and DIII-D tokamaks.

2.7 IR video bolometer

An alternative method of measuring temperature of the metal foil is to measure the infrared (IR) radiation emitted by it. The IR radiations emitted by a metal is a function of its temperature and changes as the temperature change. The IR radiations are measured using an IR camera. A prototype IR video bolometer has been successfully used in Jt-60U (Peterson et al., 2008). It has all the advantages of the metal foil bolometer, but without any electrical connection. The disadvantages of IR bolometers are slow response time and significant involvement of optics.

3. Review of bolometer diagnostic measurements

Bolometry is one of the basic diagnostics in all fusion devices. The radiation power loss measured using bolometers is crucial to the understanding of power balance of the plasma and its confinement. It also is an indication of the purity of the plasma. The radiation emission distribution and its time evolution obtained from arrays of bolometers provide information about the nature of the impurities and their transport. They can also be used to determine the nature of specific modes of operation, namely, radiative mode, detached plasmas and Marfes (multifaceted asymmetric radiation from the edge). A review of the studies carried out with bolometers is given in the following sub-sections.

3.1 Power balance of the plasma

The input power into a fusion device like tokamak can be accounted as the sum of the stored power in the hot plasma, the power conducted to the limiter/divertor or the plasma facing components and the power radiated isotropically by the hot plasma. The radiated power loss in most of the devices has been found to be a significant fraction of the input power and equals the input power in some cases. This fraction depends on the plasma parameters and also on the material of the vessel in which the plasma is contained. The parametric dependence of radiation power loss has been studied in various devices. Although no universal scaling laws have been established, general trends have been seen in many tokamaks. The radiation power loss is directly related to the plasma electron density and inversely to the toroidal magnetic field. It also has a strong dependence on the vessel conditioning and vessel material. Also, the radiation power loss data from different machines indicate variation with the size of the plasma. The larger the plasma size, the higher is the radiation power loss from it.

3.2 Radiation emission distribution

The emission of radiation is non-uniform in the plasma. The plasmas with similar total radiated power and similar conditions behave differently when the emission distributions are different. This spatial variation in emission results from the difference in the electron

temperature profile and in the type of the impurity present in the plasma. The emission distribution is obtained by using two or three arrays of bolometers that cover the entire plasma cross-section. The bolometers in the array measure line integrated radiation along different lines of sight. These measurements are then inverted using a suitable inversion algorithm to determine local emission value. In case a single array of bolometers is used, one has to make an assumption of circularly symmetric distribution. The emission distribution combined with the spectroscopic measurements give a complete picture of the impurity distribution and the behavior of the plasma.

The plasmas that have a high concentration of low-z elements (carbon, oxygen) radiate strongly at the plasma boundary. The strong emission cools the edge and hence the temperature is low near the walls. This reduces the sputtering and arcing from the wall and hence the metal concentration in the plasma. So the temperature is high in the center and the plasma channel is narrow. Such discharges have good confinement. In contrast, only high-z impurities can reach the plasma core and when the concentration of high-z impurities is significantly high, it gives rise to core cooling. As a result the temperature profile is hollow, double-tearing plasma instability arises and plasma confinement is poor.

The anomaly in the radiation profile has been seen as a precursor to the density limit disruptions in some tokamaks. In both ohmic and auxiliary heated discharges, the plasma density can only be increased up to a point when the radiated power equals the input power. As the density is increased, the radiated power also increases and hence the plasma channel shrinks. This can give rise to thermal/radiative instability and Marfe (multifaceted asymmetric radiation from edge). They have been observed in several tokamaks, for example, Textor (Rapp et al., 1999), ASDEX (Stabler et al., 1992), and JET (Behringer et al., 1986).

3.3 Physics of Marfe and detached plasma

Marfe is a radiation instability that occurs when the density of a discharge is increased in plasmas with low impurity content. The increase in the density increases the radiation power ($P = L_z (T_e) n_z n_e$), which causes edge cooling and further increase of radiation power loss. The empirical scaling shows that there is a limit to the maximum achievable density at given plasma current, which is known as the Greenwald limit, n_{Gw} (m^{-3}) = $1 \times 10^{17} I_p / \pi a^2$ (kA/m^2). When the density of the plasma is raised towards this limit, a Marfe appears. Large amount of radiation is emitted from a small region on the high field (inboard) side of the plasma edge during a Marfe. Marfe has a certain poloidal extent (~30°) above the midplane and is present at all toroidal locations. An array of bolometers that views the plasma from the top shows asymmetry in the radiation. The exact location and extent of marfe is obtained by inverting the bolometer data from bolometer arrays that view the plasma from top and side. The radiation profile gives an unambiguous picture of the Marfe location and the time profile gives its evolution. Marfes have been studied extensively in Alcator C (Lipschultz et al., 1984), JT-60 (Nishitani et al., 1990) and TFTR (Bush et al., 1988).

Detached plasmas result from a drop in the edge electron temperature below the threshold for ionization of all the plasma species. Hence, cold neutrals surround the plasma and the radiating layer is shifted to a smaller minor radius. In detached plasmas, most of the input

power is radiated from a shell at the boundary of the plasma and the power and particle fluxes to the walls are greatly reduced. Detached plasmas can be used to validate the accuracy of the bolometric diagnostics on a tokamak since the only loss channel is the radiation power loss. Another bolometric signature of detached plasma is a very steep rise in the radiated power at the plasma edge. The detached plasma regimes have been studied extensively in TFTR (Bush et al., 1988), Textor (Tokar, 1995) tokamaks, and they can be induced in order to reduce the power load on the plasma facing components.

3.4 Impurity injection for reducing heat load on the limiter and divertor

The high temperature in the thermonuclear fusion also raises the question of power exhaust at the divertor. The conducted heat loads on the limiters/divertors of the present operating devices are enormous and the ones that are expected in the next generation devices are much higher (~20 MWm^{-2}) that are impractical for any material. Thus, it is essential to device a method to reduce the heat loads. In many tokamaks, this is done by injecting trace impurities ($n_z/n_e \sim 10^{-3}$) of gases with $z \geq 10$ in the periphery of the plasma without affecting the core plasma parameters and stability. In TEXTOR (Samm et. al., 1993) and Tore Supra (Grosman, 1995), it has been demonstrated that the injection of neon enabled establishment of quasi-stationary layer that radiated 90% of the input power (Pospieszczyk et. al., 1995) from the edge. In TFTR neutral beam heated discharges trace impurity of xenon, and krypton were used to generate discharges with increased radiation power loss and decreased conduction and convection power losses to the limiter (Hill et al., 1999).

4. Examples from Aditya tokamak

We now present examples of radiation power measurements on Aditya tokamak. It is a medium sized tokamak of major radius 0.75m and minor radius 0.25m (Bhatt et al., 1989). It is in operation for two decades, and during this period various experiments have been conducted to study the edge fluctuations, turbulence and plasma instabilities. The typical operational parameters of Aditya plasmas are as follows: toroidal magnetic field on axis B_T = 0.75 T, plasma current I_p = 75-100 kA, central electron density n_e = (1-3)×10^{19} m^{-3} and central electron temperature T_{e0} = 300- 400 eV. It is equipped with all the standard diagnostics.

4.1 Bolometer system

There are two cameras for the measurement of the radiation power loss and radiation emission distribution in Aditya. One is a single channel collimated bolometer (AXUV-5), mounted on the top port that views the whole poloidal plasma cross- section (solid angle 0.16 sr). A second camera that has an array of 16 detectors (AXUV-16ELO) is mounted on the radial port and views the whole poloidal cross section of the plasma through a pinhole. The spatial resolution of this camera is 10 cm at the vessel mid-plane and the temporal resolution is 0.2 ms. The detector array and the single detector are mounted in UHV chambers and connected to the electronics in a compact housing mounted on the machine port. The electronics includes current-to-voltage convertors, amplifiers, filters and drivers for all photodiodes. The fully differential output from the electronics card is then transmitted to the data acquisition system (Tahiliani et al., 2009).

4.2 Bolometer data analysis

The AXUV detector signal (S) is related to the radiation emission in the plasma and can be written as,

$$S = G R_{res} E \int g(r)\, dl \tag{19}$$

Here, G (V/A) is amplifier gain, R_{res} (A/W) is AXUV responsivity, E (m^2) is etendue of the system , and g (Wm-3) is the emissivity, which is a function of the electron density, impurity density, and the electron temperature. The integral is along the line of sight of the detector. The line-integrated emissivity, is also called the brightness, B.

The radiation power loss P_{rad} (W) can be obtained from the measured value of B. For the single channel detector P_{rad} is given by,

$$P_{rad} = 2\pi R_0\, 2a\, B \tag{20}$$

It can also be determined from the array measurements by the following equation:

$$P_{rad} = 2\pi R_0 \sum_i B_i \Delta r_i \tag{21}$$

Here R_0 is major radius of the tokamak, a is minor radius, Δr_i is chord width at the mid-plane, and the summation is over all detectors of the array.

The line-integrated measurements B of the array detectors can be inverted using a suitable inversion algorithm to obtain emissivity (g) distribution in the plasma. In Aditya, ART (Algebraic Reconstruction Technique) is used (Tahiliani et al., 2009) along with an assumption of circular symmetry.

4.3 Experimental results

An example of measured B-profile is shown in figure 4. It is observed that radiation power loss from Aditya tokamak ranges from 20% - 40% of the input power during the current flat top and is close to the input power at the end of the discharge. It has been shown separately that the radiated power fraction (P_{rad} /P_{in}) decreases linearly with increasing current indicating that the low-z impurities are dominant since they radiate less at elevated temperatures. The variation of radiation power loss has also been studied with the electron density. It is seen that the radiated power remains constant with increasing density up to $[n_e] \sim 1.6 \times 10^{19}$ m^{-3} and thereafter it increases with the density.

The radiation emission profiles are found to be hollow with little radiation from the central part of the plasma column and a radiation peak at the edge. This is in line with the presence of low-z impurities and a very low metal concentration. With the central electron temperature of 300 – 400 eV in Aditya we expect the low-*z* impurities to be fully ionized.

We have further carried out radiation power measurements in discharges with additional short pulses of the working gas (Gas Puff, GP) as well as MBI (Molecular Beam Injection). It is observed that GP leads to an increase in the edge radiation while MBI reduces the recycling in the edge. This may indicate that GP may be used to cause radiation cooling of

the plasma edge and thereby reduce plasma instability drive that is responsible for edge fluctuation (Jha et al., 2009). On the other hand, MBI can also be used for edge modification, probably by causing velocity shear suppression of fluctuation because both seem to reduce edge recycling.

Radiation power measurements in discharges with DLD (density limit disruptions) have also been studied. It is observed that the edge detector signal increases during the disruption phase and becomes comparable to that of the central detector indicating contraction of the plasma channel. In the DLD induced by GPs we observe that the edge line-integrated radiation is about an order of magnitude higher than the core line-integrated radiation. However, because of the fact that during DLD the edge detectors saturate and there may be significant radiation loss in the wavelength range 1200 – 1500 Å, in which detector sensitivity is poor, it is not possible to estimate the radiation fraction accurately.

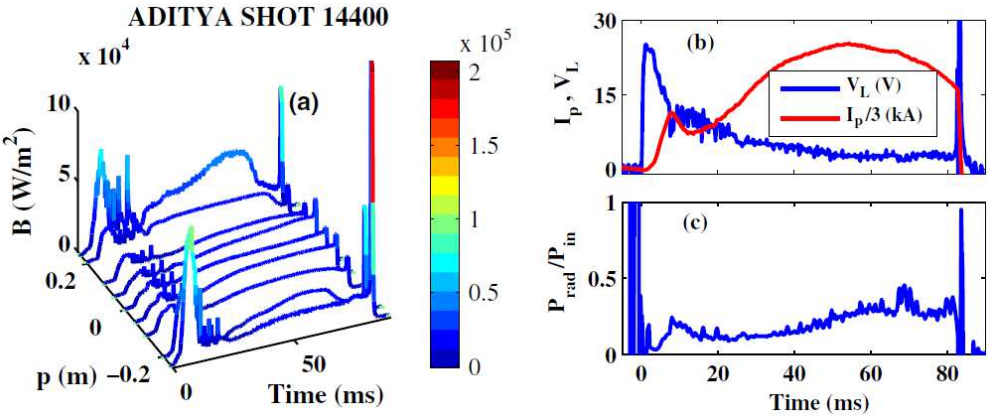

Fig. 4. (a) The brightness (B) profile of the array detectors for Aditya discharge number 14400, (b) plasma current (I_p) and loop voltage (V_L) that gives input power $P_{in}=I_pV_L$, and (c) the fraction of the radiated power (P_{rad}) to the input power P_{in}.

5. Bolometers on ITER tokamak

ITER is an international collaboration to test the feasibility of fusion and it is under construction in Cadarache, France. ITER aims to demonstrate that it is possible to produce commercial energy from fusion. The scientific goal of the ITER project is to deliver ten times the power that it consumes. From 50 MW of input power, the ITER machine is designed to produce 500 MW of fusion power—the first of all fusion experiments to produce net energy. During its operational lifetime, ITER will test key technologies necessary for the next step: the demonstration fusion power plant that will prove that it is possible to capture fusion energy for commercial use. The physics design of ITER is completed (Perkins et al., 1999) and its construction is underway.

In ITER, the use of bolometer diagnostic is two folds. The first is to measure and control the radiation power loss from the divertor region. For the sustenance of the preferred operation at high density, it is critical to control and enhance the power that is radiated from the edge

of the plasma, especially from the divertor legs and the X-point. The second is to measure the spatially resolved radiation power for the study of the power balance of the discharge. A spatial resolution of 20 cm in the main plasma and 5 cm in the divertor and X-point region is required for these tasks. Also, the proposed method for the inversion of the bolometer data is sparse data tomography, which would require 340 lines of sights of measurements (Young et al., 1999). The bolometer arrays will be installed in the equatorial and vertical ports and in the specially instrumented divertor diagnostic cassettes. From each of these locations, several arrays of detectors will observe the plasma. From the equatorial port, the inner divertor leg (high resolution) and the main plasma are viewed; from the vertical port, the main plasma, the area of the X-point, and the largest part of the divertor legs (high resolution) can be seen. This view can give the total radiation power loss.

Efforts are being made to develop and test a suitable bolometer detector that could withstand the high neutron flux and the temperature expected in ITER. The typical values of the expected neutron flux and radiation dose (mostly gamma ray) are listed in table 2. It is seen that neutral flux is five times, neutron flux is ten times and neutron fluence is 10,000 higher compared to the existing machines.

Parameters	First wall	Blanket gap (VV)
Neutron flux [$m^{-2}s^{-1}$] (>0.1 MeV) (14 MeV)	3×10^{18} 8×10^{17}	$(0.2\text{-}1)\times10^{17}$ $(0.8\text{-}4)\times10^{16}$
Fluence (>0.1 MeV) [m^{-2}]	3x1025	(0.4-2) x 1024
Dose rate [Gy/s = 100 rad/s]	2000	20-100
Neutral particle flux [$m^{-2}s^{-1}$]	5x1019	1x1018
Plasma radiation [kW m^{-2}]	500	10
Time varying mag. field [T]	1	~1

Table 2. The estimated particle and radiation load in ITER.

The most eligible candidate for ITER is the metal foil bolometer. The metal foil bolometer used on JET has a proven performance in an ITER like environment. The metal foil bolometers presently being used on JET tokamak (see table 1) have been tested and the neutron irradiation tests show that they can't survive a full lifetime of ITER due to the transmutation of gold to mercury, embrittlement of the mica or kapton foil, and the failure of the contacts. The gold has been replaced by platinum as the thermal neutron capture cross section of platinum is a factor of 10 smaller than that of gold. A new bolometer with platinum absorber (3μm) on SiN foil has been produced and tested successfully (Meister et

al., 2008). But for ITER, a bolometer foil thickness of 12μm is required to ensure absorption of X-rays with energies up to 25 keV. So efforts are being done to develop a bolometer with a thickness of 12 μm.

6. Conclusion

The bolometers are essential diagnostic for the measurement and control of the radiation power loss from the fusion plasmas. This diagnostics is used extensively both for physics studies and for operation and control of fusion plasma devices. Over the last thirty years, this diagnostics have been developed from the early use of thermister and thermopiles to the present use of absolute photodiodes and radiation hard metal foil bolometers. The present day bolometers can withstand neutron fluence up to 2.5×10^{14} cm^{-2} and radiation dose up to 10 Grad. However, the next generation fusion devices will have much higher levels of radiation doses and neutron fluence, and therefore new bolometers that work in such harsh conditions may have to be developed.

7. References

Behringer, K.H., Carolan, P.G., Denne, B.,Decker, G., Engelhardt, W., Forrest, M.J.,Gill, R.,Gottardi, N. Hawkes, N.ckalline, E., Krause, H. Magyar, G. Mansfield, M.,Mast F., Morgan, P., Peacock, N.J., Stamp, M.F. & Summers H.P. (1986). Impurity and Radiation Studies During The JET Ohmic Heating Phase. *Nuclear Fusion*, Vol.26, No.6 (1986) pp.751-768, ISSN 0029-5515

Bhatt, S.B., Bora, D., Buch, B.N., Gupta, C.N., Jain, K.K., Jha, R., John, P.I., Kaw, P.K., Kumar, Ajay, Matto, S.K., Natarajan, C., Pal, R., Pathak, H.A., Prabhakara, H.R., Pujara, H.D., Rai, V.N., Rao, C.V., Rao, M.V.V., Sathyanarayan, K., Saxena, Y.C., Sethia, G.C., Vardharajalu, A., Vasu, P. & Venkataramani, N. (1989). ADITYA: The First Indian Tokamak. *Indian Journal of Pure and Applied Physics*, Vol.27, (1989), pp. 710-742, ISSN 0019-5596

Bush, C.E. & Lyon, J. F. (1977). Wall Power Measurements of Impurity Radiation in ORMAK.*Oak Ridge National Laboratory Report,* ORNL/TM-6148, (December 1977)

Bush, C.E., Schivell, J., McNeill, D.H., Medley, S.S., Hendel, H.W., Hulse, R.A., Ramsey, A.T., Stratton, B.C., Dylla, H.F., Grek,B., Johnson, D.W., Taylor, G., Ulrikson, M. & Weiland, R.M. (1988). Characteristics of Radiated Power for Various Tokamak Fusion Test Reactor Regimes. *Journal of Vacuum Science and Technology A*, Vol. 6, No.3, (May/June 1988), pp 2004-2007, ISSN 0734-2101

Edmonds, P.H. & England A.C. (1978). Eneregy Loss To The Wall and Limiter in NormalORMAK Discharges. *Nuclear Fusion*, Vol.18, No.1 (1978), pp. 23-27, ISSN 0029-5515

Furno, I., Weisen, H., Mlynar, J., Pitts, R. A., Llobet, X., Marmillod, Ph. & Pochon, G. P. (1999)Fast Bolometric Measurements on The TCV Tokamak. *Review of Scientific Instruments*, vol. 70, No.12, (December 1999), pp. 4552-4556, ISSN 0034-6748

Gorelik, L.L., Mirnov, S.V., Nikolevsky, V.G. & Sinitsyn, V.V. (1972) Radiation Power of aPlasma as a Function of the Discharge Parameters in the Tokamak-3 Device *Nuclear Fusion* Vol.12 (1972) pp. 185-189, ISSN 0029-5515

Gray, D. S., Luckhardt, S. C., Chousal, L., Gunner G., Kellman, A. G. & Whyte, D. G., (2004)Time resolved radiated power during tokamak disruptions and spectral averaging of AXUV photodiode response in DIII-D *Review of Scientific Instruments* Vol. 75, No. 2 (Feburary 2004), pp. 376-381, ISSN *0034-6748*

Grosman, A., Monier-Garbet, P., Vallet, J.C.,Beaumont, B., Chamouard, C. , Chatelier, M.,DeMichelis, C., Gauthier, E., Ghendrih, P., Guilhem, D. , Guirlet, R. , Lasalle, J. , Saoutic, B. & Valter, J. (1995) Radiative layer control experiments within an ergodized edge zone in Tore supra. Journal of Nuclear Materials, Vol. 220-222, (April 1995), pp. 188-192, ISSN 0022-3115

Hill, K. W., Scott, S.D.,Bell, M., Budny,R., Bush, C. E., Clark, R. E. H., Denne-Hinnov, B., Ernst, D. R., Hammett, G. W. , Mikkelsen, D. R. , Mueller, D. , Ongena, J. , Park, H. K., Ramsey, A. T., Synakowski, E. J. , Taylor, G. & Zarnstorff, M. C. (1999) Tests of local transport theory and reduced wall impurity influx with highly radiative plasmas in the Tokamak Fusion Test Reactor. *Physics of Plasmas*, Vol.6, (1999), pp. 877-884, ISSN 1070-664X

Hsuan, H., Bol, K. & Ellis, R.A. (1975). Measurement of the Energy Balance in ATC Tokamak.Nuclear Fusion, Vol.15 (1975) pp. 657-661, ISSN 0029-5515

Korde, R., (2007) International Radiation Detectors Inc., Available from: <http://www.ird-inc.com>

Jensen, R.V., Post, D.E., Grasberger, W.H., Tarter, C.B. & Lokke, W.A. (1977). Calculations of Impurity Radiation and its Effects on Tokamak Experiments. Nuclear Fusion, Vol. 17, No.6, (1977), pp.1187-1196, ISSN 0029-5515

Jha, R., Sen, A., Kaw, P. K., Atrey, P. K., Bhatt, S. B., Bisai, N., Tahiliani, K., Tanna, R. L. & the ADITYA Team. Investigation of gas puff induced fluctuation suppression in ADITYA tokamak. (2009). Plasma Physics and Controlled Fusion, Vol.51, No.9, (2009), pp.17, ISSN 0741-3335

Joye, B., Marmillod, Ph. & Nowak S. (1986). Multichannel Bolometer for RadiationMeasurements on the TCA Tokamak. Review of Scientific Instruments, Vol.57, pp. 2449-2456, (1986), ISSN: *0034-6748*

Krumery, M. & Tegeler, E., (1990) Semiconductor photodiodes in the VUV: Determination of layer thicknesses and design criteria for improved devices. Nuclear Instruments and Methods in Physics Research Section A: Accelerators, Spectrometers, Detectors and Assocaited Equipment, Vol. 288, No.1, (1 March 1990), pp. 114-118, ISSN 0168-9002

Lipschultz, B., LaBombard, B., Marmar, E. S., Pickrell, M. M., Terry, J. L., Watterson, R. &Wolfe, S. M. (1984) Marfe: An Edge Plasma Phenomena. Nuclear Fusion, Vol. 24, No. 8, (1984), pp. 977-988, ISSN 0029-5515

Maeno, M. & Katagiri, M. (1980). An Application of a Germanium Film Bolometer toRadiation Loss Measurement in JFT-2 Tokamak Japanese Journal of Applied Physics, Vol.19, (1980), pp. 1433-1434, ISSN 0021-4922

Mast, K. F., Krause, H., Behringer, K., Bulliard, A. & Magyar G. (1985) Bolometric diagnostics in JET Review of Scientific Instrument, Vol. 56, (1985), pp.969-972, ISSN *0034-6748*

Mast, K. F., Vallet, J. C., Andelfinger, C. , Betzler, P. , Kraus, H. & Schramm G. (1991). A LowNoise Highly Integrated Bolometer Array for Absolute Measurement of VUV and Soft x –ray Radiation. Review of Scientific Instruments, Vol.62, (1991), pp. 744-751, ISSN *0034-6748*

Meister, H., Giannone, L., Horton, L. D., Raupp, G. , Zeidner, W. , Grunda, G. , Kalvin, S.,Fischer, U., Serikov, A., Stickel, S. & Reichle R. (2008) The ITER bolometer diagnostic: Status and plans Review of Scientific Instruments Vol. 79, (2008), pp. 10F511-10F516, ISSN *0034-6748*

Muller, E. R. & Mast F. (1984). A New Metal Resistor Bolometer for Measuring Vacuum Ultraviolet and Soft x Radiation. *Journal of Applied Physics*, Vol.55, (1984), pp. 2635-2642, ISSN 0003-6951

Nishitani, T., Itami, K.,Nagashima, K., ,Tsuji., S, Hosogane,N., YOSHIDA, H., Ando, T., Kubo, H. & Takeuchi, H. (1990) Radiation Losses and Global Power Balance of JT-60 Plasmas. *Nuclear Fusion*, Vol.30, No.6 (1990), pp. 1095-1105, ISSN 0029-5515

Odajima, K., Maeda, H., Shiho, M., Kimura, H., Yamamoto, S. , Nagami, M. , Sengoku, S., Sugie, T., Kasai, S., Azumi, M. & Shimonura Y. (1978) Radiation Loss and Power Balance in DIVA. *Nuclear Fusion*, Vol.18, No. 10 (1978) pp. 1337-1345, ISSN 0029-5515

Orlinskiz, D.V. & Magyar G. (1988). Plasma Diagnostics on Large Tokamaks. *Nuclear Fusion*, Vol.28, No.4, (1988), pp 611-697, ISSN 0029-5515

Paul, S. F., Fonck , R. J., & Schmidt, G. L. (1987). Operation of a Tangential Bolometer on the PBX Tokamak. *Princeton Plasma Physics Laboratory report,* PPPL-2432 (1987)

Perkins, F. W., Post, D.E., Uckan N.A., Azumi, M., Campbell, D.J. , Ivanov, N., Sautho, N.R., Wakatani, M., Nevins, W.M., Shimada M., Van Dam, J., Cordey G., Costley, A., Jacquinot, J. , Janeschitz, G., Mirnov, S., Mukhovatov, V., Porter, G. , Post, D., Putvinski, S., Shimada, M., Stambaugh, R., Wakatani, M., Wesley,J., Young, K., Aymar, R., Shimomura, Y., Boucher, D. , Costley, A., Fujisawa, N., Igitkhanov, Y., Janeschitz, G., Kukushkin, A., Mukhovatov, V., Perkins, F., Post, D., Putvinski, S., Rosen-bluth, M. & Wesley J. (1999). Chapter 1: Overview and summary. *Nuclear Fusion*, Vol.39, (1999), pp. 2137, ISSN 0029-5515

Peterson, B.J., Parchamy,H., Ashikawa,N., Kawashima,H., Konoshima,S., Kostryukov, A.Y.,Miroshnikov,I.V., Seo,D., & Omori T. (2008). Development of imaging bolometers for magnetic fusion reactors. *Review of Scientific Instruments*, Vol.79, (2008), pp. 10E301-10E306, ISSN *0034-6748*

Pospieszczyk, A., Samm, U., Bertschinger, G., Bogen, P., Claassen, H. A.., Esser, G., Gerhauser, H., Hey, J. D., Hintz, E., Konen, L. , Lie, Y. T. , Rusbuldt, D. , Schorn, R. P.,Schweer, B., Tokar, M., Winter, J. , the TEXTOR Team, Durodie, F., Koch,R., Messiaen, A.M., Ongena,J., Telesca, G., Vanderplas, R.E., van Nieuwenhove.R., van Oost, G., van Wassenhove, G. & Weynants (1995) R. R. Study of the power exhaust and the role of impurities in the Torus Experiment for Technological

Oriented Research (TEXTOR) Physics of Plasmas , Vol. 2, No.6, (June 1995), *I SSN: 1070-664X*

Rapp, J., De Vries, P.C., Schuller, F.C., Tokar M.Z., Biel W., Jaspers, R., Koslowski H.R., Kramer-Flecken, A.,Kreter A., Lehnen, M., Pospieszczyk, A., Reiser D., Samm U. & Sergienko G. (1999) Density Limits in TEXTOR-94 Auxiliary Heated Discharges. Nuclear Fusion, Vol. 39, No. 6 (1999) pp.765-776, ISSN 0029-5515

Sabine, G. B. (1939). Reflectivities of Evaporated Metal Films in the Near and Far Ultraviolet. Physical Review, Vol. 55, (June 1,1939) pp. 1064-1069, ISSN 1943-2879

Samm, U., Bertschinger, G., Bogen, P., Hey, J.D. , Hintz, E. , Knen, L. , Lie, Y.T.,Pospieszczyk, A., Rusbiildt, D., Schorn, R.P., Schweer, B. Tokar', M. & Unterberg B. (1993) Radiative Edges Under Control By Impurity Fluxes Plasma *Physics and Controlled Fusion*, Vol.35 (1993) pp. B167-BI75, ISSN 0741-3335

Scatturo, L.S. & Pickrell M.M. (1980). Bolometric Measurements And The Role of Radiation inAlcator Power Balance. *Nuclear Fusion*, Vol.20, No.5 (1980) pp. 527-535, ISSN 0029-5515

Schivell, J., Renda, G., Lowrance, J. & Hsuan, H. (1982). Bolometer for Measurements onHigh-Temperature Plasmas. *Review of Scientific Instruments*, Vol.53, No.10, (Oct. 1982), pp.1527-1534, ISSN *0034-6748*

Sharp, L. E., Holmes L S, Scott P E & Aldcroft D. A. (1974). A thin film thermopile for neutral particle beam measurements. *Review of Scientific Instruments* Vol.45 (1974) pp.378-381, ISSN *0034-6748*

Shimada, M., Campbell, D.J., Mukhovatov, V., Fujiwara, M.Kirneva, N., Lackner, K., Nagami, M., Pustovitov, V.D., Uckan, N. , Wesley, J., Asakura, N., Costley, A.E., Donne, A.J.H., Doyle, E.J., Fasoli A., Gormezano, C., Gribov, Y. ,Gruber, O., Hender, T.C., Houlberg, W. , Ide, S. , Kamada, Y. ,Leonard, A., Lipschultz, B., Loarte, A., Miyamoto, K., Mukhovatov, V.,Osborne,T.H. , Polevoi1, A. & Sips, A.C.C. (2007) *Nuclear Fusion,* No. 47 (2007) S1–S17, ISSN 0029-5515

Snipes, J.A., Bora, D. & Kochanski, T.P. (1984). Initial Bolometric Measurements on Text. *Fusion Research Center Technical Report* , DOE/ET/53043-T2; FRCR-269, (Dec 1, 1984)

Stabler, A., McCormick, K. , Mertens, V. , Muller, E.R. , Neuhauser, J. , Niedermeyer, H. , Steuer, K.-H. , Zohm, H. , Dollinger, F. , Eberhagen, A. , Fussmann, G. , Gehre, O. , Gernhardt, J. , Hartinger, T. , Hofmann, J.V. , Kakoulidis, E. , Kaufmann, M. , Kyriakakis, G. , Lang, R.S. , Murmann, H.D. , Poschenrieder, W. , Ryter, F. , Sandmann, W. , Schneider, U. , Siller, G. , Soldner, F.X. , Tsois, N. , Vollmer, O. & Wagner, F. (1992) Density limit investigations on ASDEX Nuclear Fusion, *Vol.32, No.9, pp* 1557-1583, ISSN 0029-5515

Tahiliani, K., Jha. R., Gopalkrishana, M. V., Doshi, K., Rathod, V., Hansalia, C. & ADITYA team. (2009) Radiation power measurement on the ADITYA tokamak. *Plasma Physics and Controlled Fusion* Vol.51 (2009) 085004 pp 13, ISSN 0741-3335

TFR group, (1980). Bolometric Technics on TFR 600. *Journal of Nuclear Materials*, Vol. 93-94,Part-1, (1980) pp. 377-382, ISSN 0022-3115

Tokar, M.Z. (1995). Non-Linear Phenomena in Textor Plasmas Caused by Impurity Radiation. *Physica Scripta*, Vol.51, pp. 665-672, (1995), ISSN: 0031-8949

Wen, Y. & Bravenec, R.V. (1995). High-Sensitivity, High-Resolution Measurements of Radiated Power on TEXT-U. *Review of Scientific Instruments*, Vol.66, pp.549-552 (1995), ISSN *0034-6748*

Wesson, J. (2004), *Tokamaks* (Third Edition), Oxford University Press,0 19 8509227, OxfordYoung, K.M., Costley, A.E., Bartiromo, R., deKock , L., Marmar, E.S., Mukhovatov, V.S.,Muraoka, K., Nagashima, A., Petrov, M.P., Stott, P.E., Strelkov, V., Yamamoto, S., Bartlett, D., Ebisawa, K., Edmonds, P., Johnson, L.C., Kasai, S., Nishitani, T., Salzmann, H., Sugie, T., Vayakis, G., Walker, C., Zaveriaev, V., Perkins, F. W. , Post, D. E. , Uckan, N. A. , Azumi, M.,Campbell, D. J. , Ivanov, N. , Sauthoff, N. R. , Wakatani M., Nevins, W. M. , Shimada, M. & Van Dam J.(1999) Chapter 7: Measurement of Plasma Parameters. *Nuclear Fusion*, Vol. 39, No. 12 (1999), pp. 2541-2575, ISSN 0029-5515

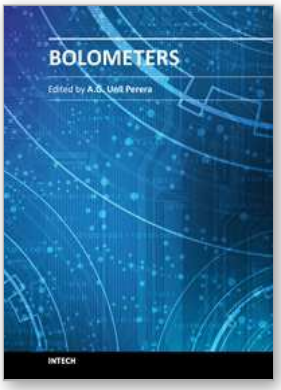

Bolometers

Edited by Prof. Unil Perera

ISBN 978-953-51-0235-9
Hard cover, 196 pages
Publisher InTech
Published online 09, March, 2012
Published in print edition March, 2012

Infrared Detectors and technologies are very important for a wide range of applications, not only for Military but also for various civilian applications. Comparatively fast bolometers can provide large quantities of low cost devices opening up a new era in infrared technologies. This book deals with various aspects of bolometer developments. It covers bolometer material aspects, different types of bolometers, performance limitations, applications and future trends. The chapters in this book will be useful for senior researchers as well as beginning graduate students.

How to reference

In order to correctly reference this scholarly work, feel free to copy and paste the following:

Kumudni Tahiliani and Ratneshwar Jha (2012). Bolometers for Fusion Plasma Diagnostics, Bolometers, Prof. Unil Perera (Ed.), ISBN: 978-953-51-0235-9, InTech, Available from: http://www.intechopen.com/books/bolometers/advances-in-bolometric-diagnostics-of-fusion-plasmas

INTECH
open science | open minds

InTech Europe
University Campus STeP Ri
Slavka Krautzeka 83/A
51000 Rijeka, Croatia
Phone: +385 (51) 770 447
Fax: +385 (51) 686 166
www.intechopen.com

InTech China
Unit 405, Office Block, Hotel Equatorial Shanghai
No.65, Yan An Road (West), Shanghai, 200040, China
中国上海市延安西路65号上海国际贵都大饭店办公楼405单元
Phone: +86-21-62489820
Fax: +86-21-62489821